

Chapter 6

Multi-step Additive Manufacturing Technologies Utilizing the Powder Metallurgical Manufacturing Route



Arne Davids, Lukas Apfelbacher, Leonhard Hitzler,
and Christian Krempaszky

Abstract Single-step additive manufacturing processes, such as laser powder bed fusion, are capable of producing metal parts within one step by full melting of the feedstock while also generating the geometric shape. However, due to high cooling rates residual stresses and related distortions pose challenges, especially in high strength materials, like tooling steels or hard metals. In multi-step additive manufacturing followed by sintering, components are produced in sequential steps divided into a shaping step achieved by additive manufacturing and a material consolidation step through sintering. Unlike in single-step processes, the material properties obtained by sintering are isotropic, and the extent of residual stresses are uncritical. Additionally, multi-step additive manufacturing is also capable of processing ceramics and metals unsuitable for welding. This review provides an overview about relevant aspects of additive manufacturing categories used in multi-step AM toward sinter-based parts, namely vat photopolymerization (VPP), material extrusion (MEX) and binder jetting (BJ). In principle, these AM technologies are generally similar in utilizing a polymeric binder material as matrix for the powder material, but due to the inherent process differences, the specifications of the binder materials differ significantly, as shown in this study.

A. Davids (✉) · L. Apfelbacher · L. Hitzler · C. Krempaszky
Institute of Materials Science and Mechanics of Materials, Technical University of Munich,
Boltzmannstraße 15, 85748 Garching, Germany
e-mail: arne.davids@tum.de

L. Apfelbacher
e-mail: lukas.apfelbacher@tum.de

L. Hitzler
e-mail: leonhard.hitzler@tum.de

C. Krempaszky
e-mail: krempaszky@tum.de

6.1 Introduction

Additive manufacturing (AM) has become a key technology for the product development process. Predominantly, additive manufacturing is used for rapid prototyping; however, it is increasingly utilized throughout the whole product development and manufacturing process. The broad use of AM technologies is derived from their potential to greatly reduce the number of manufacturing steps to fabricate prototypes or components, for which conventional technologies may need several steps (i.e., different machines, reclamping of the workpiece, tool changes, etc.) to achieve similar part complexity. Other advantages are opportunities of weight saving, material property optimization and embedded functionality without any additional costs. Single-step AM processes which fully melt the feedstock are most wide-spread based on their industrial use and conducted research. However, a downside of these processes are residual stresses and related distortions that are well-known phenomena in welding processes (DebRoy et al. 2018; Hitzler et al. 2018). Since multi-step AM processes utilize a non-metallic binder to generate the part shape and the consolidation takes place in a followed and uniform sintering process, residual stresses are far less. Other driving forces for the adaption of multi-step AM are cost reduction, material availability and continuous innovation.

The aim of the present study is to characterize the multi-step AM technologies vat photopolymerization (VPP), material extrusion (MEX) and binder jetting (BJT) and to provide an overview about their strengths and weaknesses. Apart from describing key-process characteristics, a special focus is set on used binder materials, as it plays a key role in shaping process and also influences the material properties of the final sintered part.

6.2 Metal Additive Manufacturing

Metal AM technologies use metal feedstock, such as powder, wire or metal and binder mixtures to produce three-dimensional (3D) parts by progressively adding material. According to the ISO/ASTM 52900–2022 standard, metal AM technologies can be divided into single-step and multi-step AM processes, see Fig. 6.1.

6.2.1 *Single-Step AM Technologies*

Single-Step AM technologies generate the shape and material properties simultaneously. Metal AM technologies that are considered as single-step AM processes are: powder bed fusion technologies, which fully melt the metal powder; direct energy deposition, which deposits the loose feedstock (powder or wire) together with energy for melting; and material jetting, which ejects molten metal droplets (similar to the

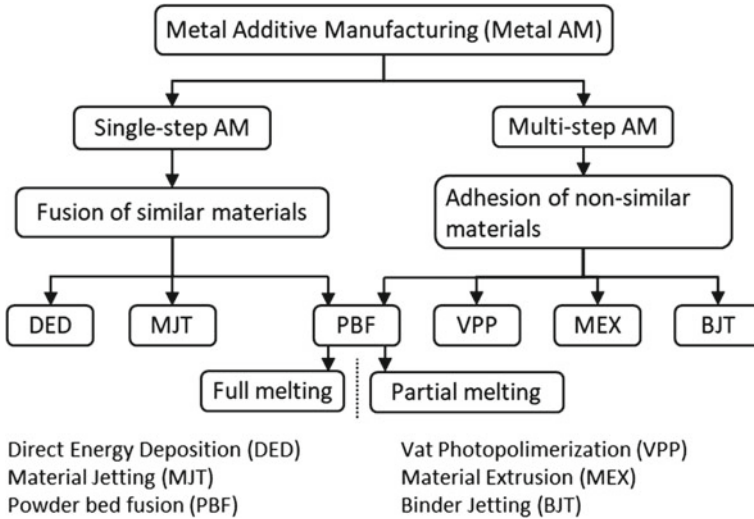


Fig. 6.1 Categorization of selected metal additive manufacturing technologies by the number of manufacturing steps needed to achieve a final metal part (DIN 2022)

inkjet principle). A significant disadvantage of most single-step AM technologies are residual stresses arising due to thermal gradients and shrinkage. These can lead to part imperfections like cracks or deformations (Sames et al. 2016).

6.2.2 Multi-step AM Technologies

Multi-step additive manufacturing technologies include two or more consecutive process steps to produce a final solid part (DIN 2022). These steps are similar to the powder metallurgical manufacturing route shown in Fig. 6.2, and include:

- (1) Shaping: Generating the part shape out of metal powder and binding media utilizing AM technologies.
- (2) Debinding: Removal of the primary binding media.
- (3) Sintering: Removal of the secondary and residual binder while consolidating the metal powder (Bartolo and Gaspar 2008; Suwanpreecha and Manonukul 2022; Ziaee and Crane 2019).

Feedstock:

The feedstock used for multi-step AM, predominantly is a premixed multi-component material, consisting of the metal powder and a binding media. The binding media needs to be specifically tailored to the AM technology. Its main purpose is to support the shaping process and to act as a matrix structure for the metal powder.

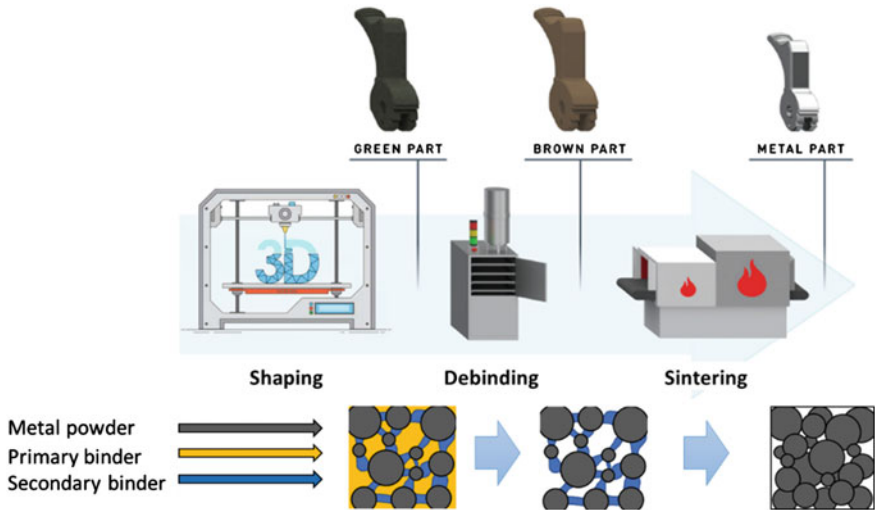


Fig. 6.2 Process scheme of multi-step additive manufacturing technologies; image adopted from (Process—PTI 2022)

The binding media consists of three components: primary binder, secondary binder and additives, such as dispersants or surfactants. The primary binder, also referred to as main binder, accounts for the majority of the volume. It is a low molecular weight polymer, which is easily removable. The secondary binder, also called backbone binder, is a high molecular weight polymer. Its purpose is to maintain the 3D printed shape after debinding and before sintering. (Suwanpreecha and Manonukul 2022).

Shaping:

During shaping, the part geometry is generated. In conventional powder metallurgical processes, this is done by pressing or injecting loose powder or a powder binder mixture into a mold. The utilization of molding techniques usually come with restrictions regarding the part shape and high manufacturing costs (Moon et al. 2021). Additive manufacturing overcomes these restrictions through the layer-by-layer manufacturing principle which allows for more complex designs and without requiring molds. Most intensively researched in that regard are vat photopolymerization, material extrusion and binder jetting processes (Vaezi et al. 2020).

Debinding:

For typical multiple-component binders, the debinding process is split into two stages: primary debinding and secondary debinding. In the first stage, the primary binder is removed. This is done by solvent debinding, immersing the additive manufactured green part into a solvent, or by thermal debinding, which degrades the polymer into volatile products. Most common solvents are water or acetone. The intermediate product is referred to as “brown part”. The secondary debinding is a transition process between debinding and sintering. While the backbone binder

degrades, sintering between the powder particle starts (Ebel 2019; Suwanpreecha and Manonukul 2022). Improper thermal debinding leads to carbonaceous residues that degrade mechanical, optical, thermal, magnetic or electronic properties of the sintered part (Heaney 2019).

Sintering:

Sintering relies on diffusion in solid matter and the principle to reach a lower energy state. Neighboring powder particles in direct contact initially develop necks between each other. This connection gradually widens during the sintering process until a dense part is achieved. At the same time, shrinkage occurs and the density of the part increases. Contrary to the shaping process in which the properties of the binding media are more influential, the sintering process predominantly depends on the metal powder and its properties. Thus, the parameters for the sintering process are material specific. Residual porosity, which is characteristic for sintered parts, can be led back to the particle size of the initial powder and correlated with the green part density. It can, further, be controlled through sintering temperature and time (Šalák 1995). Because the powder consolidation is separate from the AM process and starts uniformly from the part surface, multi-step additive manufacturing followed by sintering inherits less residual stress, compared to single-step AM (DebRoy et al. 2018).

6.2.2.1 Vat Photopolymerization (VPP)

Vat photopolymerization utilizes a liquid photo-reactive polymer, which is selectively polymerized inside a vat (DIN 2022). The process steps for VPP are as follows (detailed in Fig. 6.3): (1) The build platform is lowered into a polymer resin inside a vat, (2) the thin liquid layer gets exposed to UV light, causing the polymer to cure, (3) the build platform is raised again, so new resin flows in and forms a new liquid layer and (4) when the new liquid layer is established, the build platform immerses the last cured layer again into the liquid and the cycle repeats. Most commonly the light source is a laser or a projector system directed by mirrors (Chen et al. 2019).

Table 6.1 gives key-process parameters that can be varied to alter the desired part properties.

Feedstock:

The photo-reactive resin is comprised three components: (1) photo-initiators, which absorb the light and start the curing process, (2) monomers and oligomers, which provide photo-curability and (3) dispersants to maintain low viscosities even in presence of high powder loadings. Additional components may be added to influence the resins rheology, to enhance curability or to ease binder removal (Rasaki et al. 2021; Zimbeck and Rice 2000). For metal stereolithography processing, the typical powder loading is 50 vol-%, higher loadings are generally desirable due to multiple advantages. These include shortening of the debinding time, minimizing the porosity in the sintered part, reducing the risk of part disruption during binder decomposition

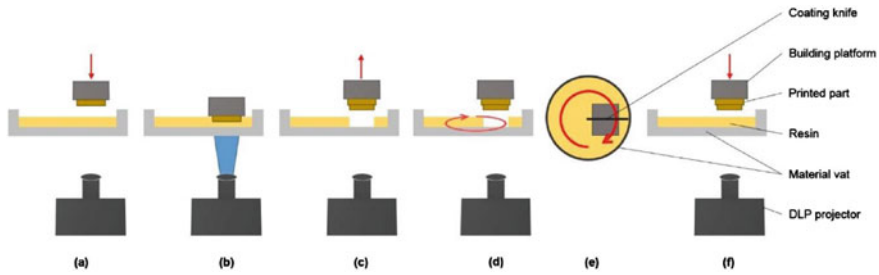


Fig. 6.3 Process steps of the VPP process. **a** Build platform with the already printed layers is immersed into the vat, **b** liquid layer is exposed to UV light and cured, **c** build platform is lifted, **d** Vat surface is recoated with fresh resin, **e** top view of the recoating procedure, and **f** process steps (a) to (e) are repeated until part is finished. Image adopted from (Stögerer et al. 2022)

Table 6.1 Key-process variables in VPP (in accordance with Oh et al. (2020)).

Part placement	Build strategy	Light exposure
<ul style="list-style-type: none"> • Orientation • Support structure 	<ul style="list-style-type: none"> • Layer height • Tool path (only Laser) • Vat temperature 	<ul style="list-style-type: none"> • Exposure duration • Exposure intensity • Light source resolution

and reducing sintering shrinkage (Zimbeck and Rice 2000). Typical resins used for metal VPP as well as powder load and debinding temperature are listed in Table 6.2.

Advantages and Disadvantages:

The biggest advantages of VPP are the high achievable surface quality and accuracy. In addition, VPP utilizes a nonhazardous and easy to handle feedstock. The metal powder is contained within the UV-reactive resin and thus avoids the issues and required safety measures related with loose metal powder. One drawback of powder-filled resins is it being a suspension with limited shelf life due to sedimentation (Zubrzycka et al. 2021). Other limitations of VPP are the rather slow build rate, the

Table 6.2 Binder systems utilized in metal VPP

Binder	Powder loading vol-%	Debinding temperature °C	References
HDDA ^a	50	600	Lee et al. (2006)
Unsaturated polyester and epoxy system	50	n.n	Bartolo and Gaspar (2008)
Acrylate monomers (Di-, tri- and higher)	52	500	Zimbeck and Rice (1998)

1,6-Hexanediol diacrylate

Table 6.3 Advantages and disadvantages of VPP

Advantages	Disadvantages
High surface quality High accuracy and resolution No loose powder handling (power suspension)	Slow build rate Parts are not stackable inside the build chamber Short shelf life of resin Part size limited

need for support structures and the small part sizes due to the restrictions of the light source (see Table 6.3) (Zhou et al. 2016).

Commercially available AM machines:

Commercial systems are available from Incus GmbH (Vienna, Austria), which offer a machine and service for producing VPP-based metal parts. The company started as a spin-off from Lithoz GmbH (Vienna, Austria) and solely focused on processing ceramic powder-filled resins with vat photopolymerization (Boissonneault 2019). Admatec BV (Alkmaar, Netherlands) also offers two systems for processing of metal-filled resins (Admaflex 130 and 300).

6.2.2.2 Material Extrusion (MEX)

The principle of material extrusion is based on the reversible effect of thermoplastic polymers, which become moldable when heated above their glass transition temperature and solidify again upon cooling. In MEX, this mechanism is used to extrude the thermoplastic feedstock through a nozzle onto a build plate and generates a three-dimensional (3D) part by depositing the extrudate onto the already solidified polymer. There are different extrusion concepts to process thermoplastic material. The three basic principles thereof are depicted in Fig. 6.4. Matching feedstock properties and the extruder principle is vital for the shaping process. In a plunger-based approach, the processed material is present in a semi-liquid slurry; therefore, process ability is predominantly driven by the viscosity. To allow easy processing of filament-based material, it is important to ensure a sufficient flexibility of the filament, so it does not break when fed to the extrusion unit. Moreover, it is essential that the cross-section of the filament is in a tight range to maintain a steady material flow. A comprehensive study about problems in filament-based MEX was undertaken by Hsiang Loh et al. (2020). In comparison with the other approaches, the requirements toward pellet material are the lowest due to fewer requirement on the feedstock.

Key-process parameters that influence print quality are listed in Table 6.4.

Feedstock:

The feedstock used in MEX processes is available as pellets, filament or slurry. The metal MEX process is rather similar to metal injection molding (MIM), and thus, the feedstock consists of similar components known from MIM. These are divided into primary polymers with a low molecular weight and secondary polymers with

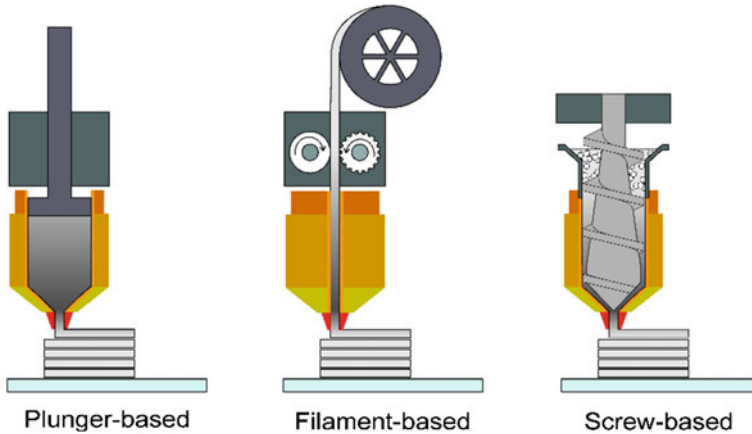


Fig. 6.4 Different extrusion concepts in material extrusion (Gonzalez-Gutierrez et al. 2018)

Table 6.4 Key-process parameter in MEX (in accordance with Oh et al. (2020)).

Part placement	Build strategy	Material extrusion
<ul style="list-style-type: none"> • Orientation • Support structure 	<ul style="list-style-type: none"> • Nozzle diameter • Layer height • Tool path • Travel speed • Build platform temperature 	<ul style="list-style-type: none"> • Volume extrusion rate • Nozzle diameter • Extrusion temperature

a higher molecular weight. Since there is no standardized definition regarding the classification of primary and secondary binder, only a general guideline is provided. Primary binders commonly are based on paraffin or synthetic wax, polyethylene glycol (PEG), thermoplastic elastomers (TPE), styrene-ethylene-butylene-styrene (SEBS) and ethylene–vinyl acetate (EVA). The following components are considered as secondary binder: Polyamide (PA), polypropylene (PP), polyethylene (PE, LDPE, HDPE) and polyoxymethylene (POM) (Kan et al. 2021). An additive that is regularly used as a lubricant is stearic acid (SE). Table 6.5 summarizes reported research on binder materials in MEX.

Advantages and Disadvantages:

The key advantage of MEX is the high material throughput (compared with VPP and BJT), that is achieved with upscaling the extrusion unit. However, this entails a loss in surface quality and resolution, due to the correlation of nozzle diameter to bead size. Since no optical components are utilized in MEX, the initial cost for this technology is lower compared to other AM technologies. Similar to VPP, the metal powder is encapsulated inside the binder material, allowing an easier and nonhazardous material handling. A disadvantage of MEX is that parts cannot be

Table 6.5 Binder materials used in MEX

Feedstock	Binder composition	Solvent debinding		Thermal debinding			References
		Solvent	Temperature in °C	Duration in h	Temperature in °C	Duration in h	
Pellets	PEG and wax	Water	60	12	500	1	Lieberwirth et al. (2017), Singh et al. (2021a)
Pellets	TPE and PP	Water and inhibitor	60	48–72	600–800		Lengauer et al. (2019)
Pellets	PEG and wax	Water	60	48–72	500	1	Singh et al. (2021b; c), Vishwanath et al. (2021)
Slurry	PEG	Water	60	10	–	–	Giberti et al. (2016)
Slurry	Embemould K83	Water	40	48	145–300	6	Hassan et al. (2021)
Filament	POM, PP and wax	–	–	–	600	2	Abe et al. (2021)
Filament	TPE and PO	Cyclohexane	70	N/A	600	N/A	Gonzalez-Gutierrez et al. (2019)
Filament	PP, SEBS wax and SA	Cyclohexane	60–70	24	350–440	1–4	Kan et al. (2021)
Filament	LDPE, TPE and SA	Cyclohexane	60	N/A	370–470	N/A	Wagner et al. (2022)
Filament	PA	–	–	–	200–450	N/A	Riecker et al. (2016)
Filament	POM and wax	–	–	–	600	2	Kurose et al. (2020)
Filament	TPE, PO and compatibilizer	Cyclohexane	60	3–12	–	–	Kukla et al. (2017)

(continued)

Table 6.5 (continued)

Feedstock	Binder composition	Solvent debinding		Thermal debinding			References	
		Solvent	Temperature in °C	Duration in h	Temperature in °C	Duration in h		Atmosphere
Filament	TPE and PO	Cyclohexane	65	0.5–57	750	1.5	Vacuum	Thompson et al. (2019)
Filament	POM, PE, DOP, DBP and ZnO (BASF Ultrafuse 316LX)	HNO ₃ gas	110–140	8	450–600	1–2	H ₂	Damon et al. (2019), Ait-Mansour et al. (2020), Liu et al. (2020), Caminero et al. (2021), Jiang and Ning (2021), Rosnitschek et al. (2021)
Filament	POM, PE, DOP, DBP and ZnO (BASF Ultrafuse 316L)	HNO ₃ gas	120	N/A	450–600	1	N/A	Jiang and Ning (2021), Quarto et al. (2021)
Filament	PE and SA	–	–	–	200–425	3	N/A	Wang et al. (2021)
Filament	Polyolefin-based	Aceton	60	24	300–550	N/A	N/A	Zhang et al. (2020)

Table 6.6 Advantages and disadvantages of MEX (Vaezi et al. 2020)

Advantages	Disadvantages
High build rate	Low surface quality
Low initial technology costs	Parts are not stackable inside the build chamber
No loose powder handling	

stacked within the build chamber and support structures are required to manufacture overhangs. This reduces the potential for mass production, due to a low exploitation of the building space and manual labor to remove supports (see Table 6.6) (Vaezi et al. 2020). Overall, the highest potential of MEX is seen in large volume components.

Commercially Available AM Machines:

AM machines based on MEX are widely available for polymer material. While it is generally possible to process highly filled metal feedstock as filament, there are only a few companies that specifically advertise the use of metal powder-filled feedstock. AIM3D GmbH (Rostock, Germany) offers with the ExAM 255 a system with two single screw extruders, capable of processing two different feedstocks (for example build material and support material) at the same time. In addition, Pollen AM (Ivry-sur-Seine, France) offers systems to produce green parts through MEX technology. With their PAM Series P, they offer a 3D printer with open software controls that processes pellet feedstock. As a provider of feedstock BASF SE (Germany) developed a filament feedstock on the basis of their Catamold system, which can be processed by many regular polymer filament 3D printers (Suwanpreecha and Manonukul 2022).

6.2.2.3 Binder Jetting (BJT)

Binder jetting (BJT) is a powder-bed-based AM technology in which a powder is deposited layer-by-layer similar to PBF and selectively joined in each layer with a binding agent that is dispensed via an inkjet printhead. The process steps are divided into three steps. In the first step, a flat powder layer is deposited on the build platform. The flattening is done by a rake or a rotating roller. The unit responsible for the powder deposition and flattening is called recoater (see Fig. 6.5). After powder deposition, a binding agent is selectively applied with a printhead. This step is very similar to the common inkjet printing in which a 2D image is printed onto the powder. Depending on the binding agent, a third step is performed to cure the binder with heat or UV-irradiation.

The part placement is less restrictive than in VPP and MEX, since no support structure is required. During the shaping process, the printed part is surrounded by the powder bed, which stabilizes it. Further, BJT requires less amount of binder to fabricate a green part, because it solely functions as a binding media and not as an auxiliary material for the process (Li et al. 2020). Since the full strength of the part is only achieved after sintering, particular caution needs to be taken to not damage the

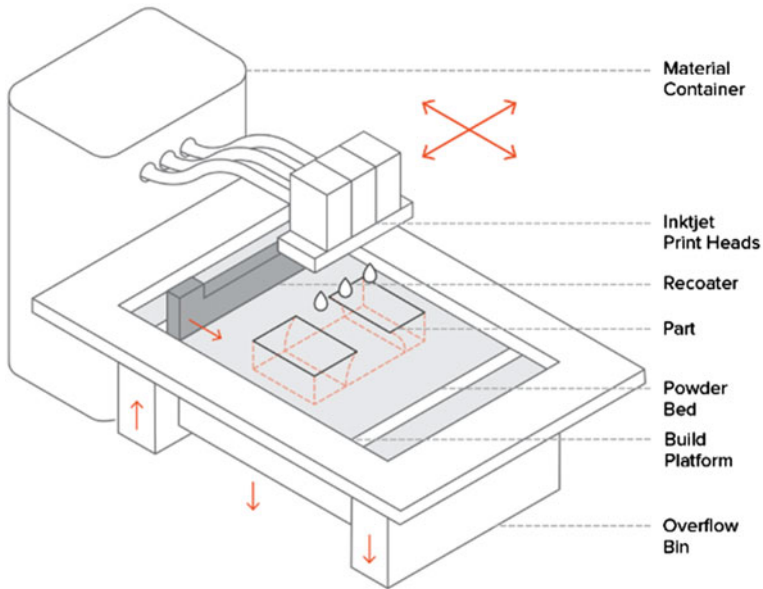


Fig. 6.5 Schematic of a binder jetting machine (3D Hubs Inc 2022)

part in advance. Therefore, recoating speed is limited due to the friction generated during the powder deposition. The main influence of the ink jetting process is on the resolution of the part. This is mostly determined by the nozzle size and the number of the inkjet printhead. When choosing the printhead, it is especially important to ensure the compatibility of the binder ink with the printhead. Table 6.7 gives key-process parameters that can be adapted toward the part geometry, powder material or ink system.

Material:

Regarding the powder deposition, the powder requirements in binder jetting are comparable to other powder bed-based processes. Similar to these, powder particle size, shape and powder bulk density influence the flowability and thus determine the recoating speed and the density of the powder layer. The selection of a suitable binder, compatible with the powder, is critical for successful printing. The two most

Table 6.7 Key-process parameters in BJT (in accordance with Oh et al. (2020)).

Part placement	Powder recoating	Ink jetting
<ul style="list-style-type: none"> • Orientation 	<ul style="list-style-type: none"> • Layer height • Blade traverse speed • Roller rotation speed 	<ul style="list-style-type: none"> • Nozzle diameter • Nozzle number • Binder saturation

important criteria are the wettability and permeation ability which affect the migration of the binder and the strength of the green part (Li et al. 2020). Due to the complexity of binder development, this study can only provide an overview of possible criteria and binder classes that assists in the decision of a binder system.

First and foremost, the binder must be printable with an inkjet printhead. The jettability of a binder is determined by its viscosity, surface tension, viscoelasticity and other properties (Tuladhar 2017). Further, the binder ink needs to be tuned to the employed printhead system. Generally, binder systems are defined as either in-liquid or in-bed binder systems. For an in-liquid solution, all binder components are mixed inside the printed agent. This allows for a greater versatility, but also increases the risk of clogging inside the printhead. An in-bed solution splits the binder components in two parts. One part is in the ink that is printed, the other part is either a solid or liquid and is premixed into the loose powder. Table 6.2 summarizes binder materials used for BJT (Table 6.8).

The binding media is of particular importance, as it needs to be suitable for both feedstock and printhead. Thus, it was observed that many reported studies use proprietary binder systems in their research.

Advantages and Disadvantages:

Table 6.8 Binder media used in BJT

Binder	Curing temperature °C	Curing time h	References
3D systems ZB60	Air dried	1	Sheydaeian et al. (2017)
DEG	200	2	Cordero et al. (2017)
DEG aqueous	100–150	4–6	Li et al. (2017), Paranthaman et al. (2016)
Dextrine/Glycerine	Air dried	24	Fu et al. (2013)
Dextrine/Glycerine	Air dried/70	24	Carrijo et al. (2016)
EG/DEG	200	2	Elliott et al. (2016)
EGBE/IPA/EG	195	2	Do et al. (2017)
EGBE/IPA/EG	195	2	Do et al. (2017)
ExOne EGME/EG	175	N/A	Mostafaei et al. (2016), Mostafaei et al. (2017)
ExOne EGME/EG	175	N/A	Mostafaei et al. (2018)
ExOne LB 04	200	2	Bailey et al. (2016)
ExOne PM-B-SR-04	200	2	Dilip et al. (2017)
ExOne PM-B-SR1-01	170	2	Sun et al. (2009)
ExOne PM-B-SR1-04	190	2	Bai and Williams (2015)
ExOne PM-B-SR2-05	190	2	Bai et al. (2015)
ExOne ProMetal R-1	200	N/A	Levy et al. (2017)
PVA/IPA	IR light	0.33	Williams et al. (2011)
PVA/PVP	Air dried	24	Xiong et al. (2012)

Table 6.9 Advantages and disadvantages of metal BJT

Advantages	Disadvantages
Great variety of processible materials Parts are stackable inside build chamber High build rate	Handling of loose powder Maintenance intensive inkjet printhead Inert atmosphere needed

BJT offers many potential advantages compared to other AM processes (see Table 6.9). It can process most materials available as powder and also combine multiple materials toward functionally graded materials by depositing different materials (Ziaee and Crane 2019). Additionally, BJT systems have a superior productivity due to their high build rate and ability to stack multiple parts on top of each other inside the build chamber. On the downside, the metal powder is present as loose powder, and thus, handling the powder poses health risks and mandates safety measures. Another specific disadvantage for binder jetting is the risk of irreversible clogging of printhead nozzles due to the binder curing inside the nozzles (Du et al. 2020).

Commercially Available AM Machines:

Desktop Metal Inc. (Burlington, USA) offers several metal and ceramic binder jetting machines ranging from a build volume of $350 \times 220 \times 50$ mm up to $800 \times 500 \times 400$ mm (Desktop Metal Inc.). Digital Metal AB (Höganäs, Sweden) offers with its DM P2500 a binder jetting 3D printer with a build volume of $250 \times 217 \times 186$ mm (Digital Metal).

6.3 Summary

In metal multi-step AM followed by sintering, components are produced in sequential steps divided into a shaping step achieved by additive manufacturing, and a material consolidation step through sintering. Unlike in single-step processes, material properties obtained by sintering are isotropic and residual stresses are uncritical. Therefore, multi-step AM present a favorable alternative for processing high strength materials, such as tooling steels or hard metals.

This study reviews the current research on multi-step AM and the fabrication of green parts comprised of binding media and metal powder, suitable for the powder metallurgical manufacturing route to achieve fully-dense metal parts. A comparison of the available and still in development situated technologies vat photopolymerization (VPP), material extrusion (MEX) and binder jetting (BJT) was undertaken. Providing an overview of key-process characteristics, this review focused on binder materials used multi-step AM. While some studies include information about the binder system and debinding process, it was observed that the main focus of investigations are correlations between used metal powder material and as-sintered part properties. Minor efforts were undertaken toward the influence of the binder system

on the green part production, the debinding process and on the as-sintered part properties. The authors of this study strongly recommend further investigation on binding media and compositions and their influence on the properties of the green part, the debinding process and the final (as-sintered) part properties.

References

- Abe Y, Kurose T, Santos MVA, Kanaya Y, Ishigami A, Tanaka S, Ito H (2021) Effect of layer directions on internal structures and tensile properties of 17-4PH stainless steel parts fabricated by fused deposition of metals. *Materials* (Basel, Switzerland), 14(2). <https://doi.org/10.3390/ma14020243>
- Ait-Mansour I, Kretschmar N, Chekurov S, Salmi M, Rech J (2020) Design-dependent shrinkage compensation modeling and mechanical property targeting of metal FFF. *Progress Add Manuf* 5(1):51–57. <https://doi.org/10.1007/s40964-020-00124-8>
- Bai Y, Wagner G, Williams CB (2015) Effect of bimodal powder mixture on powder packing density and sintered density in binder jetting of metals. University of Texas at Austin. <https://repositories.lib.utexas.edu/handle/2152/89376?show=full>
- Bai Y, Williams CB (2015) An exploration of binder jetting of copper. *Rapid Prototyping J* 21(2):177–185. <https://doi.org/10.1108/RPJ-12-2014-0180>
- Bailey AC, Merriman A, Elliott A, Basti MM (2016) Preliminary testing of nanoparticle effectiveness in binder jetting application. *Solid Free Form Fabrication 2016*
- Bartolo PJ, Gaspar J (2008) Metal filled resin for stereolithography metal part. *CIRP Ann* 57(1):235–238. <https://doi.org/10.1016/j.cirp.2008.03.124>
- Boissonneault T (2019) Lithoz spin-off Incus to unveil lithography-based metal 3D printing at Formnext. <https://www.3dprintingmedia.network/lithoz-spin-off-incus-lithography-metal-3d-printing/>
- Caminero MÁ, Romero A, Chacón JM, Núñez PJ, García-Plaza E, Rodríguez GP (2021) Additive manufacturing of 316L stainless-steel structures using fused filament fabrication technology: mechanical and geometric properties. *Rapid Prototyping J* 27(3):583–591. <https://doi.org/10.1108/RPJ-06-2020-0120>
- Carrijo MMM, Lorenz H, Filbert-Demut I, de Oliveira Barra GM, Hotza D, Yin X, Greil P, Travitzky N (2016) Fabrication of Ti₃ SiC₂ -based composites via three-dimensional printing: influence of processing on the final properties. *Ceram Int* 42(8):9557–9564. <https://doi.org/10.1016/j.ceramint.2016.03.036>
- Chen Z, Li Z, Li J, Liu C, Lao C, Fu Y, Liu C, Li Y, Wang P, He Y (2019) 3D printing of ceramics: a review. *J Eur Ceram Soc* 39(4):661–687. <https://doi.org/10.1016/j.jeurceramsoc.2018.11.013>
- Cordero ZC, Siddel DH, Peter WH, Elliott AM (2017) Strengthening of ferrous binder jet 3D printed components through bronze infiltration. *Addit Manuf* 15:87–92. <https://doi.org/10.1016/j.addma.2017.03.011>
- Damon J, Dietrich S, Gorantla S, Popp U, Okolo B, Schulze V (2019) Process porosity and mechanical performance of fused filament fabricated 316L stainless steel. *Rapid Prototyping J* 25(7):1319–1327. <https://doi.org/10.1108/RPJ-01-2019-0002>
- DehRoy T, Wei HL, Zuback JS, Mukherjee T, Elmer JW, Milewski JO, Beese AM, Wilson-Heid A, De A, Zhang W (2018) Additive manufacturing of metallic components—process, structure and properties. *Prog Mater Sci* 92:112–224. <https://doi.org/10.1016/j.pmatsci.2017.10.001>
- Digital Metal. DM P2500. <https://digitalmetal.tech/primer-line/dm-p2500/>
- Dilip J, Miyanaji H, Lassell A, Starr TL, Stucker B (2017) A novel method to fabricate TiAl intermetallic alloy 3D parts using additive manufacturing. *Defence Technol* 13(2):72–76. <https://doi.org/10.1016/j.dt.2016.08.001>

- DIN EV (2022) Additive Fertigung—Grundlagen—Terminologie (DIN EN ISO/ASTM 52900). Beuth, Berlin
- Do T, Kwon P, Shin CS (2017) Process development toward full-density stainless steel parts with binder jetting printing. *Int J Mach Tools Manuf* 121:50–60. <https://doi.org/10.1016/j.ijmactools.2017.04.006>
- Du W, Singh M, Singh D (2020) Binder jetting additive manufacturing of silicon carbide ceramics: development of bimodal powder feedstocks by modeling and experimental methods. *Ceram Int* 46(12):19701–19707. <https://doi.org/10.1016/j.ceramint.2020.04.098>
- Ebel T (2019) Metal injection molding (MIM) of Titanium and titanium alloys. In: *Handbook of metal injection molding*. Elsevier, pp 431–460. <https://doi.org/10.1016/B978-0-08-102152-1.00023-4>
- Elliott A, AlSalih S, Merriman AL, Basti MM (2016) Infiltration of nanoparticles into porous binder jet printed parts. *Am J Eng Appl Sci* 9(1):128–133. <https://doi.org/10.3844/ajeassp.2016.128.133>
- Fu Z, Schlier L, Travitzky N, Greil P (2013) Three-dimensional printing of SiSiC lattice truss structures. *Mater Sci Eng* 560:851–856. <https://doi.org/10.1016/j.msea.2012.09.107>
- Giberti H, Strano M, Annoni M (2016) An innovative machine for fused deposition modeling of metals and advanced ceramics. *MATEC Web Confer* 43:3003. <https://doi.org/10.1051/mateconf/20164303003>
- Gonzalez-Gutierrez J, Arbeiter F, Schlauf T, Kukla C, Holzer C (2019) Tensile properties of sintered 17–4PH stainless steel fabricated by material extrusion additive manufacturing. *Mater Lett* 248:165–168. <https://doi.org/10.1016/j.matlet.2019.04.024>
- Gonzalez-Gutierrez J, Cano S, Schuschnigg S, Kukla C, Sapkota J, Holzer C (2018) Additive manufacturing of metallic and ceramic components by the material extrusion of highly-filled polymers: a review and future perspectives. *Materials (Basel, Switzerland)*, 11(5). <https://doi.org/10.3390/ma11050840>
- Hassan W, Farid MA, Tosi A, Rane K, Strano M (2021) The effect of printing parameters on sintered properties of extrusion-based additively manufactured stainless steel 316L parts. *Int J Adv Manuf Technol* 114(9–10):3057–3067. <https://doi.org/10.1007/s00170-021-07047-w>
- Heaney DF (ed) (2019) Woodhead publishing series in metals and surface engineering. *Handbook of metal injection molding (Second edition)*. WP Woodhead Publishing
- Hitzler L, Merkel M, Hall W, Öchsner A (2018) A Review of metal fabricated with laser- and powder-bed based additive manufacturing techniques: process, nomenclature, materials, achievable properties, and its utilization in the medical sector. *Adv Eng Mater* 20(5):1700658. <https://doi.org/10.1002/adem.201700658>
- Hsiang Loh G, Pei E, Gonzalez-Gutierrez J, Monzón M (2020) An overview of material extrusion troubleshooting. *Appl Sci* 10(14):4776. <https://doi.org/10.3390/app10144776>
- 3D Hubs Inc (2022) How to design parts for binder jetting 3D printing. <https://www.hubs.com/knowledge-base/how-design-parts-binder-jetting-3d-printing/>
- Desktop Metal Inc. Metal family. <https://www.desktopmetal.com/metal-family/>
- Jiang D, Ning F (2021) Additive manufacturing of 316L stainless steel by a printing-debinding-sintering method: effects of microstructure on fatigue property. *J Manuf Sci Eng* 143(9), Article 091007. <https://doi.org/10.1115/1.4050190>
- Kan X, Yang D, Zhao Z, Sun J (2021) 316L FFF binder development and debinding optimization. *Mat Res Express* 8(11):116515. <https://doi.org/10.1088/2053-1591/ac3b15>
- Kukla C, Gonzales-Gutierrez J, Cano S, Hampel S (2017) Fused filament fabrication (FFF) of PIM feedstocks. *Congreso Nacional De Pulvimetalurgia Y I Congreso Iberoamericano De Conferencia (Volume: VI)*
- Kurose T, Abe Y, Santos MVA, Kanaya Y, Ishigami A, Tanaka S, Ito H (2020) Influence of the layer directions on the properties of 316L stainless steel parts fabricated through fused deposition of metals. *Materials (Basel, Switzerland)* 13(11). <https://doi.org/10.3390/ma13112493>
- Lee JW, Lee IH, Cho D-W (2006) Development of micro-stereolithography technology using metal powder. *Microelectron Eng* 83(4–9):1253–1256. <https://doi.org/10.1016/j.mee.2006.01.192>

- Lengauer W, Duretek I, Fürst M, Schwarz V, Gonzalez-Gutierrez J, Schuschnigg S, Kukla C, Kitzmantel M, Neubauer E, Lieberwirth C, Morrison V (2019) Fabrication and properties of extrusion-based 3D-printed hardmetal and cermet components. *Int J Refract Metal Hard Mater* 82:141–149. <https://doi.org/10.1016/j.ijrmhm.2019.04.011>
- Levy A, Miriyev A, Elliott A, Babu SS, Frage N (2017) Additive manufacturing of complex-shaped graded TiC/steel composites. *Mater Des* 118:198–203. <https://doi.org/10.1016/j.matdes.2017.01.024>
- Li L, Tirado A, Conner BS, Chi M, Elliott AM, Rios O, Zhou H, Paranthaman MP (2017) A novel method combining additive manufacturing and alloy infiltration for NdFeB bonded magnet fabrication. *J Magn Magn Mater* 438:163–167. <https://doi.org/10.1016/j.jmmm.2017.04.066>
- Li M, Du W, Elwany A, Pei Z, Ma C (2020) Metal binder jetting additive manufacturing: a literature review. *J Manuf Sci Eng* 142(9):Article 090801. <https://doi.org/10.1115/1.4047430>
- Lieberwirth C, Harder A, Seitz H (2017) Extrusion based additive manufacturing of metal parts. *J Mech Eng Autom* 7(2). <https://doi.org/10.17265/2159-5275/2017.02.004>
- Liu B, Wang Y [Yuxiang], Lin Z, Zhang T (2020) Creating metal parts by fused deposition modeling and sintering. *Mater Lett* 263:127252. <https://doi.org/10.1016/j.matlet.2019.127252>
- Moon AP, Dwarapudi S, Sista KS, Kumar D, Sinha GR (2021) Opportunity and challenges of iron powders for metal injection molding. *ISIJ Int* 61(7):2015–2033. <https://doi.org/10.2355/isijinternational.ISIJINT-2021-050>
- Mostafaei A, Stevens EL, Hughes ET, Biery SD, Hilla C, Chmielus M (2016) Powder bed binder jet printed alloy 625: densification, microstructure and mechanical properties. *Mater Des* 108:126–135. <https://doi.org/10.1016/j.matdes.2016.06.067>
- Mostafaei A, Toman J, Stevens EL, Hughes ET, Krimer YL, Chmielus M (2017) Microstructural evolution and mechanical properties of differently heat-treated binder jet printed samples from gas- and water-atomized alloy 625 powders. *Acta Mater* 124:280–289. <https://doi.org/10.1016/j.actamat.2016.11.021>
- Mostafaei A, Stevens EL, Ference JJ, Schmidt DE, Chmielus M (2018) Binder jetting of a complex-shaped metal partial denture framework. *Addit Manuf* 21:63–68. <https://doi.org/10.1016/j.addma.2018.02.014>
- Oh J-W, Park J, Choi H (2020) Multi-step metals additive manufacturing technologies. *J Korean Powder Metall Inst* 27(3):256–267. <https://doi.org/10.4150/KPMI.2020.27.3.256>
- Paranthaman MP, Shafer CS, Elliott AM, Siddel DH, McGuire MA, Springfield RM, Martin J, Fredette R, Ormerod J (2016) Binder jetting: a novel NdFeB bonded magnet fabrication process. *JOM* 68(7):1978–1982. <https://doi.org/10.1007/s11837-016-1883-4>
- Process—PTI (2022) <http://polymertek.com/inject/metal-mim/process/>
- Quarto M, Carminati M, D'Urso G (2021) Density and shrinkage evaluation of AISI 316L parts printed via FDM process. *Mater Manuf Processes* 36(13):1535–1543. <https://doi.org/10.1080/10426914.2021.1905830>
- Rasaki SA, Xiong D, Xiong S, Su F, Idrees M, Chen Z (2021) Photopolymerization-based additive manufacturing of ceramics: a systematic review. *J Adv Ceram* 10(3):442–471. <https://doi.org/10.1007/s40145-021-0468-z>
- Riecker S, Studnitzky T, Kieback B, Quadbeck P, Andersen O, Clouse J (2016) Fused deposition modeling—Opportunities for cheap metal AM. In: World PM2016 congress and exhibition. <https://www.epma.com/publications/euro-pm-proceedings/product/ep16-3297424>
- Rosnitschek T, Seefeldt A, Alber-Laukant B, Neumeyer T, Altstadt V, Tremmel S (2021) Correlations of geometry and infill degree of extrusion additively manufactured 316L stainless steel components. *Materials* 14(18):5173. <https://doi.org/10.3390/ma14185173>
- Šalák A (1995) *Ferrous powder metallurgy*. Cambridge Internat. Science Publ
- Sames WJ, List FA, Pannala S, Dehoff RR, Babu SS [SS] (2016) The metallurgy and processing science of metal additive manufacturing. *Int Mat Rev* 61(5):315–360. <https://doi.org/10.1080/09506608.2015.1116649>

- Sheydaeian E, Fishman Z, Vlasea M, Toyserkani E (2017) On the effect of throughout layer thickness variation on properties of additively manufactured cellular titanium structures. *Addit Manuf* 18:40–47. <https://doi.org/10.1016/j.addma.2017.08.017>
- Singh G, Missiaen J-M, Bouvard D, Chaix J-M (2021a) Additive manufacturing of 17–4 PH steel using metal injection molding feedstock: analysis of 3D extrusion printing, debinding and sintering. *Addit Manuf* 47:102287. <https://doi.org/10.1016/j.addma.2021.102287>
- Singh G, Missiaen J-M, Bouvard D, Chaix J-M (2021b) Copper additive manufacturing using MIM feedstock: adjustment of printing, debinding, and sintering parameters for processing dense and defectless parts. *Int J Adv Manuf Technol* 115(1–2):449–462. <https://doi.org/10.1007/s00170-021-07188-y>
- Singh G, Missiaen J-M, Bouvard D, Chaix J-M (2021c) Copper extrusion 3D printing using metal injection moulding feedstock: analysis of process parameters for green density and surface roughness optimization. *Addit Manuf* 38:101778. <https://doi.org/10.1016/j.addma.2020.101778>
- Stögerer J, Baumgartner S, Rath T, Stampfl J (2022) Analysis of the mechanical anisotropy of stereolithographic 3D printed polymer composites. *Eur J Mater* 2(1):12–32. <https://doi.org/10.1080/26889277.2022.2035196>
- Sun L, Kim Y-H, Kim D, Kwon P (2009) Densification and properties of 420 stainless steel produced by three-dimensional printing with addition of Si₃N₄ powder. *J Manufac Sci Eng* 131(6):Article 061001. <https://doi.org/10.1115/1.4000335>
- Suwanpreecha C, Manonukul A (2022) A review on material extrusion additive manufacturing of metal and how it compares with metal injection moulding. *Metals* 12(3):429. <https://doi.org/10.3390/met12030429>
- Thompson Y, Gonzalez-Gutierrez J, Kukla C, Felfer P (2019) Fused filament fabrication, debinding and sintering as a low cost additive manufacturing method of 316L stainless steel. *Addit Manuf* 30:100861. <https://doi.org/10.1016/j.addma.2019.100861>
- Tuladhar T (2017) Measurement of complex rheology and jettability of inkjet inks. In: *Handbook of industrial inkjet printing*. John, pp. 409–430. <https://doi.org/10.1002/9783527687169.ch22>
- Vaezi M, Drescher P, Seitz H (2020) Beamless metal additive manufacturing. *Materials* 13(4). <https://doi.org/10.3390/ma13040922>
- Vishwanath AS, Rane K, Schaper J, Strano M, Casati R (2021) Rapid production of AZ91 Mg alloy by extrusion based additive manufacturing process. *Powder Metall* 64(5):370–377. <https://doi.org/10.1080/00325899.2021.1911457>
- Wagner MA, Hadian A, Sebastian T, Clemens F, Schweizer T, Rodriguez-Arbaizar M, Carreño-Morelli E, Spolenak R (2022) Fused filament fabrication of stainless steel structures—from binder development to sintered properties. *Addit Manuf* 49:102472. <https://doi.org/10.1016/j.addma.2021.102472>
- Wang Y, Zhang L, Li X, Yan Z (2021) On hot isostatic pressing sintering of fused filament fabricated 316L stainless steel—evaluation of microstructure, porosity, and tensile properties. *Mater Lett* 296:129854. <https://doi.org/10.1016/j.matlet.2021.129854>
- Williams CB, Cochran JK, Rosen DW (2011) Additive manufacturing of metallic cellular materials via three-dimensional printing. *Int J Adv Manufact Technol* 53(1–4):231–239. <https://doi.org/10.1007/s00170-010-2812-2>
- Xiong Y, Qian C, Sun J (2012) Fabrication of porous titanium implants by three-dimensional printing and sintering at different temperatures. *Dent Mater J* 31(5):815–820. <https://doi.org/10.4012/dmj.2012-065>
- Zhang Y, Bai S, Riede M, Garratt E, Roch A (2020) A comprehensive study on fused filament fabrication of Ti-6Al-4V structures. *Addit Manuf* 34:101256. <https://doi.org/10.1016/j.addma.2020.101256>
- Zhou M, Liu W, Wu H, Song X, Chen Y, Cheng L, He F, Chen S, Wu S (2016) Preparation of a defect-free alumina cutting tool via additive manufacturing based on stereolithography—optimization of the drying and debinding processes. *Ceram Int* 42(10):11598–11602. <https://doi.org/10.1016/j.ceramint.2016.04.050>

- Ziaee M, Crane NB (2019) Binder jetting: a review of process, materials, and methods. *Addit Manuf* 28:781–801. <https://doi.org/10.1016/j.addma.2019.05.031>
- Zimbeck W, Rice R (2000) Stereolithography of ceramics and metals. In: IS&T's 50th annual conference. <https://www.semanticscholar.org/paper/Stereolithography-of-Ceramics-and-Metals-Zimbeck-Annapolis/8d14d3abab6c5ce9fa589932f3329f4342613d46>
- Zimbeck WR, Rice RW (1998) Freeform fabrication of components with designed cellular structure. *MRS Online Proc Libr* 542(1):165–176. <https://doi.org/10.1557/PROC-542-165>
- Zubrzycka P, Radecka M, Graule T, Stuer M (2021) Metal cation complexes as dispersing agents for non-aqueous powder suspensions. *Ceram Int* 47(13):18443–18454. <https://doi.org/10.1016/j.ceramint.2021.03.168>